

## Supplementary Appendix for “Theory of the flow-induced deformation of shallow compliant microchannels with thick walls”

by Xiaojia Wang and Ivan C. Christov

### A. Moderate thicknesses and effect on the boundary conditions

Consider a configuration similar to that shown in figure 1 but the thickness of the top wall is not as large. (The side walls are still considered very thick, specifically infinite for the purposes of this discussion.) In this moderate-thickness case, the plane strain assumption is valid as long as the deformation is small enough, but the boundary conditions imposed at the sidewalls are not clear because  $\sigma_{xx}$  is not negligible. Specifically, it is not necessarily correct to impose the simply supported boundary conditions from section 3. At the same time, there is no good reason to impose clamped boundary conditions, as the previous studies on microchannels with thinner, plate-like walls [16, 28, 29], because for the geometry considered herein the side surfaces are allowed to deform, while they were assumed to be rigid in those previous studies.

To understand the type of support at the side walls in the moderate-thickness case, we start from the free body diagram in figure 9(b). Then, the reaction forces at the sidewalls are

$$T_s = p(z)h_0, \quad N_s = \frac{1}{2}p(z)w, \quad M_s = \frac{1}{2}p(z)(h_0^2 - wd), \quad (\text{A } 1)$$

where  $T_s$ ,  $N_s$ , and  $M_s$  denote the tension, shear force and the moment respectively. Here  $d$  is introduced to represent the point of the reaction force at the bottom of the side solid. Since  $h_0 \ll w$ , we expect that  $d \ll w$  due to stress concentration. Within the top wall, the resultant tension,  $T$ , shear force,  $N$ , and moment,  $M$ , are expected to be:  $T \sim T_s$ ,  $N \sim N_s$ ,  $M \sim p(z)w^2/2 + M_s \sim p(z)w^2(1 + \delta^2 - d/w)/2 \sim p(z)w^2/2$ . Hence, we neglect  $M_s$  in the following analysis.

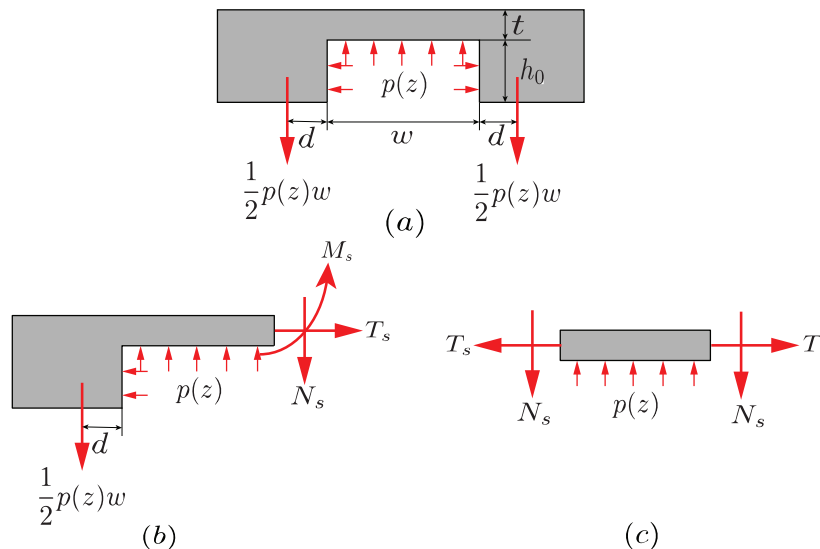


Figure 9: The force systems in the cross-section of the elastic solid's wall for moderate thickness.

Thus, we can consider the configuration from figure 9(c), a slender rectangle subject to pressure at the bottom, and shear and tension forces at the sidewalls. Note that the Airy stress function is

still applicable in this case, but it is challenging to solve the corresponding biharmonic equation (3.4) with the inclusion of tension. Fortunately, the thinness of the structure makes Saint-Venant's principle applicable, which states that "a local force system has negligible effect on the stress distribution at distances that are large compared with the dimension of the surface where the forces are applied" [52]. Accordingly, the displacement field can be estimated based on a classic engineering model, without knowing the exact details of the stress distribution in solid. Thus, we regard the top wall as a simply supported beam with tension and solve for the displacement field by extending Timoshenko's beam theory.

Mechanical equilibrium requires that

$$\frac{\partial T}{\partial x} = 0, \quad T \frac{\partial^2 u_y^0}{\partial x^2} + \frac{\partial N}{\partial x} + p(z) = 0, \quad -\frac{\partial M}{\partial x} + N = 0 \quad (\text{A } 2)$$

where  $u_y^0$  now represents the deflection of the mid-plane of the beam ( $y = t/2$ ). The deformation at the fluid–solid interface is believed to be very close to that of the mid-plane due to the slenderness of the top wall. The corresponding constitutive relations are

$$M = -\bar{E}_Y I \frac{\partial \varphi}{\partial x}, \quad N = \kappa t G \left( -\varphi + \frac{\partial u_y^0}{\partial x} \right), \quad (\text{A } 3)$$

where  $I = t^3/12$  is the second area moment of the beam cross-section,  $\varphi$  represents the rotation of the normal of the cross-section, and  $\kappa$  is the shear correction factor [53]. As before, assuming zero displacement, as well as negligible moment at  $x = \pm w/2$ , the boundary conditions are

$$u_y^0|_{x=\pm w/2} = 0, \quad M|_{x=\pm w/2} = 0. \quad (\text{A } 4)$$

Equation (A 2)<sub>1</sub> shows that the tension is constant in the cross-section, i.e.,  $T = T_s = p(z)h_0$ . Then, equations (A 2) – (A 3) can be rewritten in terms of  $\varphi$  and made dimensionless:

$$\frac{\partial^4 \varphi}{\partial X^4} - \zeta P(Z) \left[ \frac{\partial^2 \varphi}{\partial X^2} - \frac{(1+\bar{\nu})}{6\kappa} \left( \frac{t}{w} \right)^2 \frac{\partial^4 \varphi}{\partial X^4} \right] = 0. \quad (\text{A } 5)$$

Here the constant  $\zeta = Tw^2/(\bar{E}_Y I) = \mathcal{P}_0 h_0 w^2/(\bar{E}_Y I)$  has been introduced to quantify the tension effect. In equation (A 5), the first term represents the bending effect. The terms in the bracket represents the influence of tension, and the thickness effect is captured by the second term. Given the typical range of parameters for a microchannel, we conclude that the tension cannot be neglected here. Therefore, for the small thickness case, the top wall can no longer be regarded as a simply supported rectangle but, rather, it behaves like a beam with an immovable edge, i.e., simple support plus tension [54].

Solving equations (A 2) – (A 3), the vertical displacement of the mid-plane, which is also approximately the vertical displacement at the fluid–solid interface, is found to be

$$u_y^0(x, z) = \left[ \frac{w^2}{4u^2(z)h_0} - \frac{(1+\bar{\nu})t^2}{6\kappa h_0} \right] \left\{ \frac{\cosh[2u(z)x/w] - 1}{\cosh u(z)} - 1 \right\} - \frac{1}{2h_0} \left( x + \frac{w}{2} \right) \left( x - \frac{w}{2} \right), \quad (\text{A } 6)$$

where

$$u^2(z) = \frac{p(z)h_0 w^2}{4\bar{E}_Y I} \left[ \frac{1}{p(z)h_0/(\kappa t G) + 1} \right] = \frac{\zeta P(Z)}{4} \left[ 1 + \frac{(1+\bar{\nu})}{6\kappa} \left( \frac{t}{w} \right)^2 \zeta P(Z) \right]^{-1}. \quad (\text{A } 7)$$

If  $(t/w)^2 \ll 1$ , then  $u^2(z) \approx \zeta P(Z)/4 = p(z)h_0 w^2/(4\bar{E}_Y I)$  and the second term in the bracket in equation (A 6) also vanishes, then equation (A 6) is reduced to the Euler–Bernoulli beam with tension [54]. However, unlike equations (3.14)<sub>2</sub> and (3.15) of the large-thickness case, the deflection profile in equation (A 6) no longer displays self-similarity along the flow-wise direction because  $p(z)$  cannot be factored out.

To get a sense of the tension effect, we compare this proposed moderate-thickness theory with other models in figure 10. Note that we compare  $\delta H(X, Z)/P(Z)$ , with  $\delta H(X, Z) = u_y^0(x, z)/w$ , to show the magnitude of the deformation. For the applicability of linear elasticity, we expect that

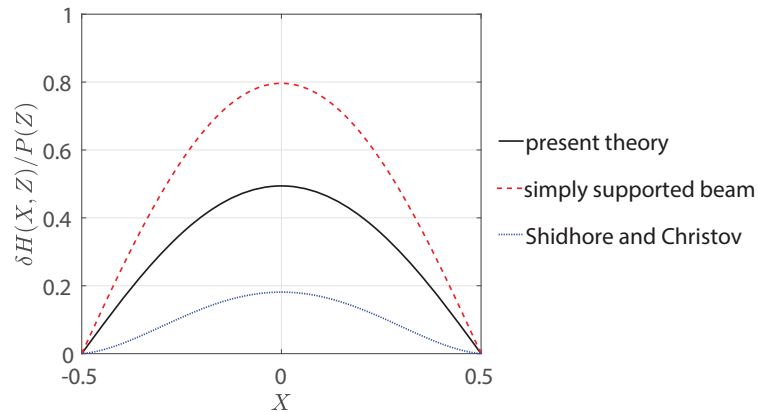


Figure 10: The cross-sectional deformation profile  $\delta H(X, Z)/P(Z)$  versus  $X$  for a microchannel with  $\delta = 0.1$  and  $t/w = 0.1$  under a pressure drop such that  $\zeta = 5$ . The solid curve corresponds to equation (A 6). The dashed curve represents the deformation of a simply supported beam using equation (3.14)<sub>2</sub>. For comparison, the dotted curve is the solution from Shidhore and Christov [29] for a clamped thick-plate-like wall.

$\delta H(X, Z) \ll 1$ . We can see that tension suppresses deformation, compared to the case of simply supported beam. However, the tension is not as restrictive as the clamping considered in [29].

As before, the flow rate–pressure drop relation is obtained by integrating the axial fluid velocity across the cross-section. Then, we rewrite  $p(z)$  as a function of  $u(z)$ , so that equation (4.1) can be written entirely in terms of  $u$ :

$$p(z) = \left[ \frac{h_0 w^2}{4E_Y I u^2(z)} - \frac{1}{\varkappa \gamma G} \right]^{-1} \Rightarrow q = - \frac{1}{12\mu} \frac{du}{dz} \frac{dp}{du} \underbrace{\int_{-w/2}^{+w/2} [h_0 + u_y^0(x, z)]^3 dx}_{=\mathcal{R}(u)}. \quad (\text{A } 8)$$

Using separation of variables, the solution of the last ODE can be expressed as a quadrature:

$$q = \frac{1}{12\mu(l-z)} \int_0^{u(z)} \mathcal{R}(u') du', \quad (\text{A } 9)$$

where  $u'$  is a “dummy” integration variable. Unfortunately, this integral can only be evaluated numerically.